Interuniversity Research Centre
on Local and Regional Finance

CIFREL Working Papers

Urban NO2 Pollution and Health Outcomes: Natural-Experiment Evidence on the Predicted Benefits of the EU Zero-Emission-Vehicles Resolution

Daniele Bondonio, Paolo Chirico,
Massimiliano Piacenza, Simone Robbiano

Working Paper n. 02/2024

CIFREL is an Interuniversity research centre that conducts applied research on local and regional governments and more generally on public economics.
The current members of the Centre are: the Department of Economics and Finance of the Università Cattolica del Sacro Cuore, the Department of Economics and Finance of the University of Brescia, the Department of Economics and Finance of the University of Ferrara, the Department of Economics and Business (DISEI) and the Department of Law and Political, Economic and Social Sciences (DIGSPES) of the University of Piemonte Orientale, the Department of Economics and Statistics Cognetti de Martiis and the Department of Economics, Social Studies, Applied Mathematics and Statistics of the University of Torino.

Contacts:

CIFREL
Università Cattolica del Sacro Cuore
Via Necchi 5
20123 Milano
Telephone: 0039.02.7234.2976
e-mail: dip.economiaefinanza@unicatt.it
web: https://centridiricerca.unicatt.it/cifrel_index.html

Urban NO_2 Pollution and Health Outcomes: Natural-Experiment Evidence on the Predicted Benefits of the EU Zero-Emission-Vehicles Resolution[*]

Daniele Bondonio[†], Paolo Chirico[†], Massimiliano Piacenza[†], Simone Robbiano[‡]

Abstract

In March 2023, the EU approved a zero-emission mobility resolution, which mandates zero CO_2 emissions for all new vehicles by 2035. This measure has sparked a heated debate due to its uncertain effectiveness in reducing pollution and CO_2 emissions globally. Nevertheless, the shift towards zero-emission vehicles has the potential to decrease local nitrogen dioxide (NO_2) pollution, particularly in urban areas where air quality is a major concern for citizens' health. This study investigates what may be the predicted impact of the EU zero-emission mobility policy on local NO_2 levels, using the draconian stay-home provision of the Italian Covid-19 lockdown of early 2020 as a natural experiment which generated an exogenous fossil-fuel-traffic abatement that proxies the implementation of the resolution. We exploit data from the urban areas with elevated traffic density in the Po-river valley in Northern Italy, a region with the highest peaks of air-pollution in Europe, and we develop a novel intertemporal statistical matching approach which is uniquely suited for policy evaluations on air-quality outcomes in the context of multivariate time series data. The results from our causal inference analysis show that Covid-19 lockdown led to a mean NO_2 reduction of 13.62 $\mu g/m^3$ (around 53% from a baseline average level of 25.8 $\mu g/m^3$). According to medical literature, this decline in NO_2 translates into a reduction in the relative risk of total, cardiovascular, and respiratory mortality of about 9%, 8%, and 4%, respectively. Moreover, we find a marked heterogeneity in the estimated impact of lockdown on pollution and health, with greater decreases in NO_2 and in the relative risk of mortality observed for higher baseline pollution levels. These findings suggest that the EU 2035 resolution is indeed expected to improve local air quality and citizens' health in urban areas with high traffic density. The estimated benefits, however, are likely to vary across EU regions based on prevailing local meteorological conditions and urban texture features, which determine a different baseline pollution, supporting the rationale for a spatial differentiation of the EU zero-emission mobility policy.

JEL classification: C10; H23; I18; Q53; R41; R48.

Keywords: Air pollution; EU zero-emission mobility policy; Urban areas, NO_2 abatement; Health effects; Intertemporal statistical matching; Impact heterogeneity.

[*] We wish to thank Elisabetta Cappa, Anthony T. Lo Sasso, Laura Magazzini, Ellen R. Meara, Fabio Padovano, Paolo Paruolo, Lorien Sabatino, Luigi Siciliani, Meiping Aggie Sun, Gilberto Turati, and all seminar participants at the *2024 Empirical Health Economics Workshop* (Sant'Anna School of Advanced Studies, Pisa), the *14th Workshop of the Network of the Economics of Regulation and Institutions* (University of Naples Federico II), the *28th Conference of the Italian Health Economics Association* (Sapienza University of Rome), the *2023 NetCIEx Workshop* (EC Joint Research Center, Ispra), and the *34th Conference of the Italian Society of Public Economics* (University of Verona), for their helpful remarks on preliminary drafts of this paper. This research did not receive any specific grant from funding agencies in the public, commercial, or not-for-profit sectors. We wish to confirm that there are no known conflicts of interest associated with this publication and there has been no significant financial support for this work that could have influenced its outcome. We also thank Giuseppe Gruttad'Auria, Andrea Nigido, Giulia Pasculli, and Michela Rosselli for their contribution in the data acquisition process.

[†] Department of Law, Economics, Political and Social Sciences (DIGSPES), Via Cavour 84 – Palazzo Borsalino, 15121 Alessandria (AL), Italy (email: daniele.bondonio@uniupo.it; paolo.chirico@uniupo.it; massimiliano.piacenza@uniupo.it).

[‡] **Corresponding author**: Department of Economics (DIEC), Via Vivaldi 5 – Darsena, 16126 Genova (GE), Italy (email: simone.robbiano@economia.unige.it).

1. Introduction

It is common knowledge that human health and ecosystems are harmed by air pollution. According to the European Environment Agency, a considerable amount of Europe's population does not live in a healthy environment but, on the contrary, in urban areas where air quality regulations are often violated. In particular, over the past decades several European regions have surpassed one or more of their emission limits for major air pollutants, i.e. ozone (O_3), nitrogen dioxide (NO_2), and particulate matter (PM), leading to major health concerns.[1]

Indeed, air pollution endangers public health in both the short and long term, including eye, nose, and throat discomfort, as well as upper respiratory diseases such as bronchitis and pneumonia; long-term health consequences may include chronic respiratory illness, lung cancer, heart disease, and even brain, nerve, liver, or kidney damage. These undesired effects caused by air pollution can necessitate costly medical treatments, resulting in high health-care expenditures, reduced productivity at work, and social welfare implications, costing millions of euro each year.

In this context, a large body of the literature has extensively documented the magnitude and importance of the adverse impact of air pollution on children and adults health (Portney and Mullahy 1986, 1990, Nafstad et al. 2004, Currie et al. 2005, 2009a, Samakovlis et al. 2005, Jerrett et al. 2005, Graff Zivin and Neidell 2009, Agarwal et al. 2010, Lleras-Muney 2010, Moretti and Neidell 2011, Pestel and Wozny 2021), mortality rates (Knittel et al. 2016, Barreca et al. 2021, Greenstone and Hanna 2014), hospital admissions (Neidell 2004, Dominici et al. 2006, Jayaraman 2008, Namdeo et al. 2011, Rava et al. 2011, Lagravinese et al. 2014), and other socio-economic outcomes, such as school performances (Currie et al. 2009b), human capital (Graff Zivin and Neidell 2013), labour supply (Hanna and Oliva 2015) and social welfare (Proost and Van Dender 2001). Therefore, to get on a sustainable path, Europe must be bold and go beyond the present environmental legislation. Indeed, many air pollutants have been significantly reduced throughout Europe during the last decades, resulting in improved air quality in such an area. However, air pollution concentrations remain too high and air quality problems persist, so that this is still an important concern for urban policies, which deserves adequate attention by policymakers at local, national and supra-national level.

In December 2019, the EU adopted a package of proposals aimed to reach no net emissions of greenhouse gasses by 2050, i.e. the European Green Deal, in order to turn Europe into the first climate-neutral continent.[2] To achieve this objective, in July 2021 the "Fit For 55" package has been proposed, including measures to make the EU's climate, energy, land use, transportation, and taxation policies capable of decreasing net greenhouse gas emissions by at least 55% by 2030 compared to 1990 levels.[3] Within the scope of this package, various proposals in the transportation sector are also included, such as a steady reduction in CO_2 emissions from vehicles and vans to "zero emissions" in 2035; this would mean that no new automobiles, whether diesel, gasoline, or hybrid, will be sold beyond that date.[4] The package of measures adopted by the EU has generated a broad debate among policymakers, stakeholders and practitioners, mainly related to uncertainties regarding an effective generalized reduction of pollution and CO_2 emissions throughout the Union; for instance, there are many concerns

[1] See https://www.eea.europa.eu/themes/air/intro.

[2] See https://commission.europa.eu/strategy-and-policy/priorities-2019-2024/european-green-deal/delivering-european-green-deal_en#transforming-our-economy-and-societies.

[3] See https://ec.europa.eu/commission/presscorner/detail/en/ip_21_3541.

[4] The measure excludes internal-combustion engine's vehicles powered by synthetic electrofuels (e-fuels), which are manufactured by means of captured carbon dioxide or carbon monoxide, together with hydrogen obtained from sustainable electricity sources such as wind, solar and nuclear power, which are CO_2-neutral.

regarding the possibility that the lower emissions of pollutants achievable with this type of mobility could be nullified by an increase in emissions related to the production of electricity (which is not always generated from renewable sources), as well as the possibility that the climate footprint of zero-emission mobility, considering the entire life cycle of a vehicle, may not be sufficient in supporting the environmental goals set by the EU.

Less controversial, instead, are the potential benefits at the local level associated with a shift toward zero-emission vehicular traffic, which could improve air quality in the most densely populated and polluted urban areas. In these areas, reducing local air pollution will benefit citizens' quality of life and health, and it constitutes a relevant policy goal.[5] For this reason it is important to assess to what extent this type of EU mobility regulation is expected to actually contribute to the abatement of local air pollution in problematic urban areas, focusing, in particular, on the benefits in terms of reduction of NO_2 local pollution. Indeed, exposure to such a pollutant has specifically been linked to increased mortality in several epidemiological studies (e.g. Faustini et al. 2014, WHO 2005); in addition, apart from carbon monoxide, NO_2 is the only widely regulated contaminant that in urban areas originates mostly from fossil fuel combustion produced by vehicular traffic.[6] In particular, Faustini et al. (2014), relying on a random-effects meta-analysis, argue that the effect on total mortality associated to an increase of 10 μg/m^3 in the annual NO_2 concentration, for European countries, is a relative risk of 1.066 (95% CI 1.029–1.104); moreover, the NO_2 effects on cardiovascular mortality and respiratory mortality have been estimated in 1.059 (95% CI 1.032-1.086) and 1.029 (95% CI 1.013-1.045), respectively.[7] This means that a similar reduction in NO_2 exposure would result in about a 7% reduction in the relative risk of total mortality, a 6% reduction in the relative risk of cardiovascular mortality, and a 3% reduction in the relative risk of respiratory mortality.

In this paper we investigate what may be the predicted impact of the "Fit For 55" EU resolution – in particular the zero-emission mobility objectives – in terms of benefits from NO_2 urban air pollution reduction, and related health outcome improvements, in one of the largest most polluted region of Europe. This is the Po-river valley in Northern Italy, which encompasses some of the most industrialized and densely-populated regions of Europe, with a total population of about 14.8 million residents, an average density of 252 inhabitants per square kilometre, and a systemic lack of sustained ventilation due to its specific orographic features (the area is almost entirely surrounded by mountain ranges) that contribute to very high peaks of air-pollution (Coker et al. 2020).[8]

[5] See, among others, Gibson and Carnovale (2015), who argue that policies aimed to reduce or eliminate private cars in urban areas are effective in reducing air pollution.

[6] Indeed, while NO_2 is mainly formed from the oxidation of nitrogen monoxide (NO) which is produced by combustion processes (such as that of fossil fuel vehicles), among the important sources of the particulate matter (both PM_{10} and $PM_{2.5}$) there are also the residues from the wear of the road surface, brakes and car tires. For this reason, when assessing air quality effects of the EU zero-emission mobility resolution, it is more proper to refer to the achievable benefits in terms of NO_2 pollution abatement, since this policy only forbids the circulation of fossil fuel vehicles and not car traffic at all.

[7] Faustini et al. (2014) also point to that the magnitude of the long-term effects of NO_2 on mortality is at least as important as that of $PM_{2.5}$, and when considering bi-pollutant analyses, with $PM_{2.5}$ and NO_2 included in the same model, the estimated impact of NO_2 shows minimal changes, suggesting that the role of NO_2 is independent of that of particles. The authors then conclude that any health impact assessment of air quality relying only on $PM_{2.5}$ and not considering NO_2, would neglect some seriously adverse effects of today's air pollution mixture.

[8] According to the expanding body of research in urban economics that assesses the impact of agglomeration on environmental conditions, when population density rises, pollutant concentrations will rise as well (Ahlfeldt and Pietrostefani, 2019, Borck and Schrauth, 2021). In particular, Ahlfeldt and Pietrostefani (2019), based on a comprehensive summary of the quantitative literature on the economic effects of density, argue that a log-point increase in urban density leads to 0.13 (log-point) higher pollution concentrations. Furthermore, Borck and Schrauth (2021) highlight that for NO_2, which has an elasticity of 0.25, and particulate matter, which has an elasticity of 0.08, the concentration rises with density. With an elasticity of 0.14, the O_3 concentration drops as density increases (see also Hilber and Palmer 2014). Finally, Carozzi and Roth (2023) find evidence in

In order to gather data that cover a period of sharp abatement of fossil-fuel vehicular traffic, mimicking the scenario of implementing the Fit For 55" resolution, we exploit the occurrence of the Italian national Covid-19 lockdown of the first half of 2020. Because of the high death toll in Italy in the early stages of the Covid-19 pandemic, the ensuing Italian lockdown has been one of the longest and most stringent in all of Europe and most of the Western world, with a mandatory at-home-stay order continuously enforced from March 10th to May 17th, 2020, and a complete closing of schools, universities, and all non-essential services and production activities.

For these reasons, a reliable estimate of the causal impact of the Italian Covid-19 lockdown on air pollution in Northern Italy has substantial importance and external validity in evaluating the local air-quality gains that could be achieved through policies (such as the "Fit For 55" EU resolution) aimed at drastically reducing fossil-fuel vehicular traffic in urban areas with systemically-high concentrations of air pollutants.

The data used in the analysis are obtained from 77 different measurement stations of the Regional Environmental Agencies (ARPA, i.e. Italian public administration entities operating in each Region of Italy and forming part of the National System for Environmental Protection) belonging to the five NUTS-2 regions located along the Po-river valley (Piedmont, Lombardy, Emilia-Romagna, Veneto, Friuli Venezia Giulia). The focus on NO_2 outcomes is because this air pollutant is linked to severe human health impacts, including respiratory and cardiovascular diseases (e.g. Niepsch et al. 2022), and it is the type of pollutant that is most prominently and specifically related to the local fossil-fuel vehicular traffic intensity (e.g. ISPRA 2021), particularly in urban areas with unfavourable orographic characteristics, with highest concentrations consistently recorded in close proximity of highly trafficked major roads (Carslaw et al. 2019, Restrepo 2021). Fort these reasons, reductions in NO_2 pollution recorded locally in densely-populated urban areas is the air-quality outcome with the highest potential of being positively affected by policies aimed to reduce fossil-fuel vehicular traffic.

Our empirical analysis mainly relates to the wide and rapidly expanding literature on the effects of environmental policies on air quality, which concentrates on regulations that specifically apply to local urban areas, such as traffic bans and low emission zones (Wolff 2014, Viard and Fu 2015, Gehrsitz 2017, Gu et al. 2017, Han et al. 2020, Rivera 2021, Sun et al. 2022), road pricing policies and/or mileage taxation (Gibson and Carnovale 2015, Luechinger and Roth 2016, Fu and Gu 2017, Green et al. 2020, Domon et al. 2022), restrictions on gasoline content and the use of diesel-powered engines (Mayeres and Proost 2001, Auffhammer and Kellogg 2011, Li et al. 2020), as well as specifically targeted air quality policies (Barron and Torero 2017, Deschenes et al. 2017, Wang et al. 2019, Rangel and Vogl 2019, Isaksen 2020, Chen et al. 2022).[9]

Our paper also contributes to the emerging strand of studies that credited Covid-19-related lockdown policies with improvements in air quality (e.g. Almond et al. 2021, Zhang et al 2021, Brodeur et al. 2021, Huang et al. 2021, Dang and Trinh 2021, Ghasempour et al. 2021, Chen et al. 2021 and Blackman et al. 2023). None of these latter studies, however, is adequate to offer a reliable empirical test on the

favor of an economically and statistically significant pollution density elasticity of 0.14 (see also Palmgren et al. 1996, Parry 2007, Parry and Timilsina 2010, Holland et al. 2016).

[9] Policies to improve mass public transport also play a key role in improving urban air quality. Indeed, the growing challenges of pollution and traffic congestion need the development of a paradigm of sustainable mobility, particularly in major cities. To this end, policies aiming at increasing the quality and accessibility of public transportation networks may be used to exert indirect control over these negative externalities associated with private transportation (e.g. Abrate et al. 2009, Chen and Whalley 2012, Lalive et al 2018, Borck 2019, Gendron-Carrier et al. 2022). See also Bento et al. (2014) for a discussion about the effects of transport regulation in the presence of multiple unpriced externalities.

perspective potential benefits of the EU zero emission vehicles resolution, because of the lack of a high stringency of considered lockdown policies, the sharp differences of the Asian and US entropic and orographic context with respect to European regions, the type of air pollutant considered in the analysis (Particulate Matter – PM – versus NO_2), and the location of the measuring stations in areas being prone to pick-up air-pollution emissions from sources substantially different from vehicular traffic.

Our causal-inference analysis on the NO_2 impact of Italian Covid-19 lockdown, is implemented by developing a novel intertemporal statistical matching (SM) approach estimated with a Malhalanobis Distance (MAHD) specification. Building on Bondonio and Chirico (2024), this approach exploits the unique impact identification conditions related to the Covid-19 lockdown and air pollution in terms of the availability of multiple multivariate time-series, one for each air-pollution measurement station, with units of observations represented by the days in which air pollution and weather characteristic are measured. Within these multivariate time-series, the abrupt change in the secular trend brought by the lockdown-induced sharp decrease in traffic is the treatment of interest, while all the major confounding factors to be controlled for, mainly in terms of weather characteristics, are observable in the data and exogenous to the treatment status (lockdown/non-lockdown) and they can be safely assumed of not being subject to unobserved secular trend (within the short pre- and post-treatment periods of times considered in the analysis). Under these conditions, our intertemporal SM approach matches, separately for each air-pollution measurement station, the single lockdown (treated) days with the non-lockdown (untreated) days that share the same control variables in terms of the most relevant weather characteristics, as regards the influence on air pollution concentration. Because the matching is implemented conditional on the same measuring station, our intertemporal SM approach yields local impact estimates (one for each measuring station) that are subsequently globally aggregated and grants a complete balancing between the treated and untreated days of the locational characteristics of the measuring stations and weather characteristics.

Intertemporal SM offers a number of advantages with the respect to the empirical strategies adopted in the recently-emerging literature on the air-quality impact of Covid-19 lockdowns. Indeed, a part of this literature does not adequately address the issues of accurate causal inference, which necessitates, above all, a good controlling of any changes in the distribution of meteorological features of pre-lockdown days and lockdown days (treatment units).[10] Other studies adopt parametric panel-data multiple regression (MR) models, that have to address the issue of error autocorrelation and require strong functional form assumptions with respect to the way in which the observable confounding factors affect air-pollution.[11] Compared to these models, our intertemporal SM design shares the same well-known advantages of SM estimation, with respect to parametric MR estimation, in terms of significantly reducing the sensitivity of the estimated impacts to the functional form that links the effects of the controls on the outcome variable (e.g. Dehejia and Wahba 2002, Iacus et al. 2011). Compared to RDD-in-time estimations, finally, our intertemporal SM approach entails the advantage of avoiding the potential for chance bias that may arise from randomly distributed daily weather characteristics into the treatment (lockdown) and comparison (pre-lockdown) period, but with small sample sizes of the calendar days across the lockdown cut-off date. This latter factor may entail a chance unbalance of the crucial confounding

[10] See, among others, Anil and Alagha (2020), Collivignarelli et al. (2020), Seo et al. (2020) and Arregocés et al. (2021).
[11] See He et al. (2020), Dang et al. (2021), Song et al. (2021) and Wang et al. (2021).

factors, unless the key confounders are explicitly measured and carefully matched between the lockdown and pre-lockdown period.[12]

The main empirical findings from our analysis show that the Covid-19 lockdown, on average, resulted in a significant drop in daily average NO_2 levels amounting to -13.62 μg/m^3, corresponding to a 53% reduction from a baseline average value of about 25.8 μg/m^3. In terms of heterogeneous impacts, our results show that the magnitude of the estimated NO_2 reduction is higher the higher it is the baseline NO_2 pollution, with estimated impacts that vary linearly, ranging from –0.18 μg/m^3 for the lowest baseline pollution (i.e. 0-10 μg/m^3) to –62.16 μg/m^3 for the highest baseline pollution (i.e. 100-150 μg/m^3). These results are robust to an extensive sensitivity analysis and placebo tests and provide empirical support to the prediction that a significant reduction in local NO_2 pollution is obtainable by future policies aimed at reducing fossil-fuel vehicular traffic, such as the EU 2035 zero-emission resolution, particularly in areas with prevailing daily meteorological conditions favourable to high levels of NO_2 pollution.

With reference to the findings from the pertaining medical literature (Faustini et al. 2014), the estimated NO_2 reductions translate into an average decrease in the relative risk of mortality of about 9% for all causes, 8% for cardiovascular causes, and 4% for respiratory causes. In terms of heterogeneous impacts, the estimated NO_2 drops translate into decreased risks of mortality ranging from 0.12% (all causes), 0.11% (cardiovascular causes), and 0.05% (respiratory causes) for the days with the lowest baseline pollution (i.e. 0-10 μg/m^3), to about 41% (all causes), 37% (cardiovascular causes), and 18% (respiratory causes) for the days with the highest baseline pollution (i.e. 100-150 μg/m^3).

These results have important policy implications and provide policymakers with some useful insights into the marginal environmental and health benefits of the EU 2035 regulation, against which to compare the opportunity cost of taxpayers' money needed to implement the green revolution and the ecological transition, as well as the welfare loss due to changes in the European automotive industry and its supply chain. Moreover, because the estimated NO_2 reduction and associated health benefits brought by the fossil fuel traffic abatement are estimated to be linearly increasing along with the baseline pollution level, our results suggest that the expected local health benefits of the EU resolution are likely to be smaller in the EU regions with prevailing daily meteorological and local urban texture conditions favourable to the dispersion of NO_2 pollution, and larger in the regions with a high incidence of unfavourable conditions (i.e. higher baseline NO_2 level). This finding provides a strong rationale for considering the introduction of some spatial policy heterogeneity in the application of fossil fuel traffic abatement resolutions, on the base of the prevailing baseline NO_2 urban pollution of the different EU regions.

The reminder of the study is organized as follows. Section 2 illustrates the impact identification properties of intertemporal SM. Section 3 details the data and intertemporal SM specifications for estimating the reduction in NO_2 pollution caused by the fossil-fuel traffic abatement brought by the Covid-19 Lockdown. Section 4 shows the empirical results, in terms of average treatment effect, placebo tests, heterogeneous impacts and additional sensitivity analysis. Section 5 translates estimated impacts of NO_2 reduction into health outcomes. Section 6 provides concluding remarks.

[12] This is in the same vein as chance bias may occur even in randomized experiments when in the presence of small sample sizes, unless stratified randomization is adopted ensuring that the known major confounders are balanced between the treatment and control group. See Section 3 for additional discussion.

2. Impact identification properties of intertemporal statistical matching

Let $\{Y_t\}$ be a stochastic process (e.g. average daily level of air pollution recorded in a given measuring station) on which a treatment (e.g. policy intervention) produces effects for a finite period L_1. The average effect of the treatment in the period L_1 is then definable as:

$$\mathrm{E}\left[Y_t^{(1)} - Y_t^{(0)} | t \in L_1\right] = \frac{1}{n(L_1)} \sum_{t \in L_1} \mathrm{E}\left(Y_t^{(1)} - Y_t^{(0)}\right) \tag{1}$$

where $n(L_1)$ is the number of time units (e.g. days) in L_1; $Y_t^{(1)}$and $Y_t^{(0)}$are the potential outcomes in case of treatment and no treatment, respectively. This average effect (1) can be considered as an *intertemporal* version of the standard *Average Treatment effect on the Treated* (ATT) (Imbens 2004, Imbens and Rubin 2015).

Because $Y_t^{(0)}$ is not observable in the interval L_1 , the intertemporal ATT (1) can be estimated under a standard *conditional mean stationery* assumption:

$$\mathrm{E}\left[Y_t^{(0)} \middle| X_t = x_t\right] = \mathrm{E}\left[Y_{t'}^{(0)} \middle| X_{t'} = x_t\right] \; \forall \; t \in L_1, t' \in L_0 \tag{2}$$

where, $\{X_t\}$ is a multivariate process of observable covariates (e.g. the weather controls), and L_0 is the finite control period which precedes L_1.

Consistent with assumption (2), the estimate of $\mathrm{E}\left[Y_t^{(0)}\right]$, given the information set $I = \{(y_t, x_t): t \in (L_1 \cup L_0)\}$, is the average of the y-observations of the time-units $t' \in L_0$ matched to the time unit $t \in L_1$ using the matching criterion $x_{t'} = x_t$, i.e.:

$$\widehat{\mathrm{E}}\left[Y_t^{(0)} | I\right] = \bar{Y}(S_{0,t}) \tag{3}$$

where

$$S_{0,t} = \{t' \in L_0 : x_{t'} = x_t\} \tag{4}$$

is the set of the time-units of L_0 matched to the time unit t of L_1.

Because the exact matching criterion (4) becomes quite limiting the greater is the number of covariates X_t and the smaller is the width of the L_0 interval, similarly to the case of the standard (cross-sectional) SM, the estimation of intertemporal ATTs can be also implemented either with Mahalanobis Distance (MAHD) matching or Propensity Score (PS) matching.[13]

In the MAHD matching , the set $S_{0,t}$ is composed of the unit/s of L_0 closest to t based on the Mahalanobis distance:

$$d_M(t, t') = \sqrt{(x_t - x_{t'})' S_X^{-1} (x_t - x_{t'})} \tag{5}$$

[13]See Rubin (1980) and Dehejia & Wahba (2002), respectively.

where S_X is the covariance matrix of the covariates calculated in $(L_1 \cup L_0)$; $(x_t - x_{t'})$ is the column vector of the differences between x_t and $x_{t'}$. While, in the PS matching, $S_{0,t}$ is composed of the unit/s of L_0 closest to t with regard to a propensity score function $\psi(x_t)$, defined as:

$$\psi(x_t) = P(t \in L_1, | X_t = x_t) \tag{6}$$

For the latter case of intertemporal PS matching, in addition, the required *conditional mean stationery* assumption is to be expressed with respect to the propensity score function $\psi(X_t)$:

$$\mathrm{E}\left[Y_t^{(0)} \middle| \psi(x_t) = \psi_t\right] = \mathrm{E}\left[Y_{t'}^{(0)} \middle| \psi(x_{t'}) = \psi_t\right] \; \forall \; t \in L_1, t' \in L_0 \tag{7}$$

Under the above framework, following Bondonio and Chirico (2024), the intertemporal ATT can be then estimated by the following matching procedure:

I. Holding constant a same time series of daily observations generated from a same cross-sectional unit (e.g. air-pollution measuring station), each day of L_1 is matched with the day(s) of L_0 of the same series having the most similar X_t;

II. For each day in L_1 on common support, a counterfactual outcome $y_t^{(0)}$ is estimated as the mean of Y-values of the corresponding matched day(s) from L_0;

III. The intertemporal ATT is estimated as:

$$\widehat{ATT} = \frac{1}{n(S_1)} \sum_{t \in S_1} \left[y_t - \hat{y}_t^{(0)}\right] \tag{8}$$

where S_1 is the set of the time-units of L_1 actually matched to time units of L_0; [14]

IV. The estimated ATT is validated if an adequate balancing is achieved and tested for the covariates X of the days in the intervention period L_1 and those of the matched control days in L_0;

V. When the analysis focuses on multiple multivariate time-series, the procedure (I)-(IV) is repeated separately for each time-series, yielding a series of local ATTs one for each multivariate time series) that are then averaged-out to a global ATT estimate.

Compared to the panel-data MR models adopted elsewhere in the literature of Covid-19 lockdowns (Dang et al. 1999, He et al. 2021, Seo et al. 2020, Song et al. 2021, Wang et al. 2021), such an intertemporal matching approach shares the same well-known advantages (e.g. Dehejia and Wabba 2002, Rosenbaum and Rubin 1983) of the standard statistical matching (SM) approaches in strongly diminishing the sensibility of the estimated impacts to the choice of functional form that links the effects of the controls on the outcome variable. Compared to RRD-in-time, our intertemporal matching approach is more efficient (granting larger external validity) and better suited to handle the potential of chance unbalancing due to the small sample size of treated units (i.e. the lockdown calendar days). This is because, holding constant the same seasonal period, main daily confounding factors (i.e. meteorological covariates) erratically distribute at random on the specific single dates around the cut-off (due to random daily occurrences of Atlantic weather fronts, African high-pressure systems, artic-

[14] Depending on the matching criterion used, some time units of L_1 may not be matched with any time units of L_0, i.e. $n(S_1) \leq n(L_1)$.

air fronts etc.), without any monotonic decreasing of the balancing of such confounders when considering calendar days further away from the cut-off. Under this circumstance, while any RDD-in-time model would obviously pass the standard no-treatment manipulation test at the threshold, it would be still vulnerable to chance bias caused small sample sizes (Lee 2008, Lee and Lemieux 2010 and Bondonio 2022), requiring to control for the absence of chance unbalancing between the treatment units (i.e. lockdown dates) and the controls (i.e. pre lockdown dates). In this scenario, our intertemporal SM approach offer a more straightforward and transparent balancing of the main confounders for all of the lockdown days, even away from the cutoff date, without risking any unnecessary restriction of the estimation sample to the dates within narrower bandwidths across the cut-off date.

3. Causal-effect estimation of Covid-19-lockdown on NO_2 pollution in Northern Italy

Our intertemporal SM procedure described in the previous section is applied to estimate the causal effect of the Italian Covid-19 national lockdown of March-May 2020 on the urban air pollution measurements from the Po-river valley area which encompass the Northern Italy regions of Piedmont, Lombardy, Emilia-Romagna, Veneto, and Friuli Venezia Giulia. These regions represent the most industrialized and densely-populated area of Italy (with an average density of 252 inhabitants per km^2). Because of these characteristics, and the specific orographic features of the Po-river valley (which is entirely surrounded by mountain ranges, except from its far east side that borders the Adriatic see), some of the highest levels of air-pollution in Europe are consistently recorded in this area (ISPRA 2021, EEA 2022). The focus on the Po-river valley area, therefore, is strategic to enlarge the external validity (and the policy-relevance) of the analysis, by enabling the recording of a large variation in the baseline NO_2 pollution, which ranges from the low levels recordable in the days with heavy precipitations and/or strong sustained wind, to the very high levels of the days with little ventilation and no precipitations.

3.1. Data

The NO_2 air pollution data used in the empirical application are collected from 77 different measurement stations of the Regional Environmental Agencies (ARPA) located along the Po-river valley within the regions of Piedmont, Lombardy, Emilia-Romagna, Veneto, Friuli Venezia Giulia (Figure 1). All of these measurement stations are located in central urban areas in close proximity with vehicular traffic and residential/office buildings, and away from power plants, industrial sites, and airports. In particular, variations in pollution from power plants are likely to be not a significant biasing factor in our spatial context, because the central urban areas where all the ARPA measuring stations are located are away from these power plants, with an average distance of 32 kilometers.[15]

Being NO_2 a pollutant from fossil-fuel combustion with very little dispersion away from its source (e.g. Chaney et al. 2011, Anttila et al. 2011, Dragomir et al. 2015, Bachtiar et al. 2017), these locational features of the measurement stations ensure that the possible recordable sources of NO_2 pollution in our data are solely vehicular traffic or fossil-fuel-combustion from heating systems and hot-water production in residential/office buildings.

[15] For all measurement stations, the minimum distance from power plants, industrial sites, and airports greatly exceeds what in the literature is estimated to be the maximum range of standard significant NO_2 dispersion away from its source of origin (i.e. 450 meters). See, e.g., Chaney et al. (2011), Dragomir et al. (2015), Bachtiar et al. (2017).

Figure 1. Spatial location of the air-pollution measurement stations

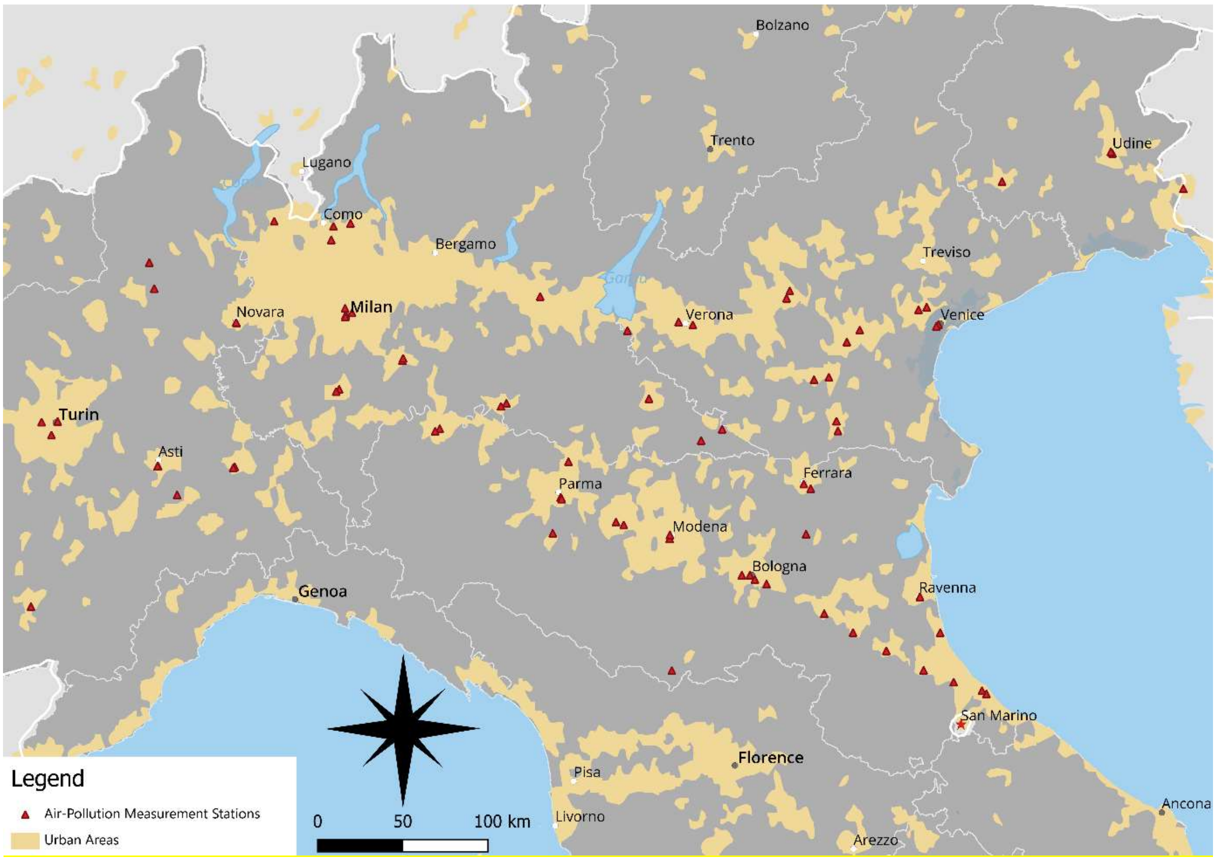

Source: Authors' elaboration via QGIS software.

In this latter regard, however, data from the Ministry of the Environment and Energy Security in the National Energy Balance suggest a zero-sum game, in which higher domestic consumption largely offset the reduction in commercial buildings, so that the Italian Covid-19 lockdown determined an increased permanence at home that was equally compensated by a corresponding absence from office buildings.[16] This entails that, in the central urban locations around the measurement stations, the potential increase in fossil-fuel consumption from the heating (and hot-water production) of residential buildings was equally compensated by a decrease consumption from the heating (and hot-water production) of office buildings, with a net-zero effect of the lockdown in terms of fossil fuel combustion unrelated to vehicular traffic. For these reasons, an important feature of our data is the possibility to interpret the estimated causal effect of the Covid-19 lockdown in terms of the impact of the abrupt abatement of fossil-fuel vehicular traffic.

The central urban location of all 77 ARPA measuring station is within municipalities characterized by elevated vehicular traffic density, with a pre-Covid-19 average of 237 registered vehicles per km of road (std. dev. 122, 10th percentile 146, median 191, 90th percentile 354)[17]. Such a modestly–dispersed distribution of municipality-level traffic density translates into specific daily baseline NO_2 pollution levels, with a much larger variation based on both the daily meteorological characteristics and the

[16] See https://www.arera.it/dati-e-statistiche?ambito=30&keyword=&settore=2&orderby=.
[17] Source: Ministry of Infrastructures and Transportation and ISTAT – Public Register of Motor-vehicles). Missing data for 23 municipalities were imputed based on the density of the nearest municipality with similar population density and vehicle per-capita figures. Excluding the imputed data, the resulting traffic-density distribution remains very similar: average 224 vehicles per km of road, median 187, 10th percentile 139, 90th percentile 391.

micro-locational urban texture of the surroundings of the measuring stations (prevalence of major boulevards, average width of the streets, presence/absence of canyoning effects due to attached buildings of the same height, etc.). Indeed, considering the 365 days preceding the start of 2020 lockdown (i.e. from March 10th, 2019 to March 9th, 2020), the average daily baseline NO_2 pollution recorded in the 77 measuring station is equal to 28.7 μg/m³, with a std. dev of 18.6 μg/m³, while the 10th percentile, the median and the 90th percentile are 9.0 μg/m³, 25.1 μg/m³ and 51.7 μg/m³, respectively. Quite a similar distribution of the daily baseline NO_2 pollution is also recorded for the 69-days period of 2019 corresponding to the 2020 lockdown (i.e. from March10 to May 17, 2019): average 25.8 μg/m³, std. dev. 16.4 μg/m³, 10th percentile 8.6 μg/m³, median 22.2 μg/m³, 90th percentile 47.2 μg/m³.

The extraordinary stringency of the mandatory-stay home provision of the Italian lockdown (in addition to the complete closures of any order of schools, universities, retailers, and all non-essential services and production activities), determined a fossil-fuel vehicular-traffic abatement which can be estimated to be around 80-90% in the Po-river valley regions in which the measuring stations are located.[18] Since in 2020 the percentage of non-fossil-fuel vehicles circulating in northern Italy was negligible (with an estimated 2.2% value), these unique circumstances entails that our impact evaluation analysis is well suited to empirically predict the local NO_2 air-quality gains that can be achieved by future policies, such as the 2035 EU Zero Emission Vehicles Resolution, for which similar reductions of fossil-fuel traffic are expected. In this latter regard, indeed, due to a residual quota of phasing-out and exempted fossil-fuel vehicles which will be still circulating also after 2035, the estimated percentage reduction of Italian fossil-fuel traffic expected by the EU resolution is within very similar ranges (75%-90%) to that of the 2020 Italian Lockdown (Isprambiente 2022).

The specific period of observation considered for our intertemporal SM estimation is the entire length of the Italian nationwide Covid-19 lockdown: 69 days from March 10 to May 17, 2020 (i.e. the intervention period L_1), together with the 365 days that preceded the start of the lockdown (the control period L_0). A longer L_0 period was instead ruled out due to the possibility that it could entail the existence of time trends that invalidate the stationarity of $\{Y_t\}$ given X_t.

The data used in the analysis also include a set of control variables (X_t) that capture the main meteorological characteristics that are known in the literature to influence air pollution: average daily temperature (TEMP), rainfall (RAIN), maximum daily wind speed (WIND) recorded in correspondence to the air-pollution measuring stations (Dang et al. 2021, Grange et al. 2018, Lovrić et al. 2021, Song et al. 2021, Wang et al. 2021). The resulting database is in terms of 77 different multivariate time series (one for each ARPA measuring station).

Table 1 compares (pooling the data from all 77 different stations and considering the daily observations with fully available data) the distribution of NO_2 recorded during the 2020 Covid-19 lockdown period with that of the same identical period in 2019. While the difference in fossil-fuel activities between the two periods is the treatment of interest, not to be controlled for in the analysis, these descriptive statistics, obviously, do not provide a reliable indication of the causal effect of the lockdown on air-pollution because of the lack of controlling for the possible differences in the distribution of the

---

[18] Arneodo et al. (2021) estimate a 90% reduction in inter-provincial mobility for the Piemonte region, and they document, for the city of Turin, a drastic decrease in average vehicle flows, entry flows in the Restricted Traffic Zone and average parking occupancy. Agresti et al. (2020), focusing on the Lombardia region and the metropolitan area of Milan, estimate an overall 77% reduction for vehicular traffic from cars and motorbikes, while for the city of Bologna and the Veneto region, an estimated 80% vehicular-traffic reduction is reported in the study by Gualtieri et al. (2020) and in a report by the Municipality of Verona (https://www.comune.verona.it/nqcontent.cfm?a_id=69423&tt=verona_agid).

meteorological variables. Indeed, as shown in Table 2, the lockdown period of 2020, for example, experienced less than half of the rain than the corresponding period of 2019.

Table 1. NO_2 levels during 2020 lockdown vs. same period of 2019 (µg/m³)

Variable	Period	Obs.	Mean	Std. Error.	95% C.I.	
NO_2	Lockdown 2020	5175	15.51	0.16	15.20	15.82
	Same period 2019	5157	25.82	0.23	25.37	26.27

Notes: Although both the lockdown and the corresponding 2019 periods are composed by exactly the same number of days, the available pooled observations from the 77 measuring stations are slightly different due to the presence of few randomly-distributed dates in which, due to technical malfunctioning of the equipment, either the NO_2 pollution or some of the meteorological characteristics could not be measured at some specific measuring station.

Table 2. Meteorological conditions during 2020's lockdown vs same period of 2019

Variable	Period	Obs.	Mean	Std. Dev.	95% C.I.	
WIND (m/s)	Lockdown 2020	5175	2.13	0.02	2.10	2.17
	Same period 2019	5157	2.24	0.02	2.20	2.28
	Difference		*-0.10*	*0.03*	*-0.16*	*-0.05*
RAIN (mm)	Lockdown 2020	5175	1.34	0.07	1.20	1.49
	Same period 2019	5157	2.69	0.10	2.49	2.89
	Difference		*-1.34*	*0.12*	*-1.59*	*-1.10*
TEMP (c°)	Lockdown 2020	5175	13.79	0.06	13.67	13.90
	Same period 2019	5157	12.57	0.04	12.50	12.65
	Difference		*1.22*	*0.07*	*1.08*	*1.35*

3.2. Average-treatment-effect estimation

In terms of Average Treatment effects on the Treated (ATT), the first step in the implementation of the intertemporal SM estimation is the exclusion (within each multivariate time series from the 77 different ARPA measuring stations) of the days in the control period L_0 that are outside of the common support for the meteorological characteristics X_t. The causal effect of the Covid-19 lockdown on the average level of NO_2 is then estimated by means of an intertemporal Mahalanobis Distance (MAHD) matching specification, replicated with a Propensity Score (PS) intertemporal matching specification used as part of the sensitivity analysis tools, together with a Random Forest Regression (RFR) model.

For estimating both the main model, in terms of MAHD matching, and the PS matching and RFR used in the sensitivity analysis, the meteorological covariates also include a set of lagged terms capturing the weather characteristics (WIND, RAIN, TEMP) of the previous day (t-1). This is in line with the data operationalization choices adopted elsewhere in the literature on Covid-19 lockdown and air pollution (Dang et al. 2021, Lovrić et al. 2021, Wang et al. 2021), and it is a solution that is justified on the base of descriptive statistics on the data showing that the daily air-pollution values of any given location may indeed be affected also by the condition of the previous days (particularly if the latter are in terms of heavy rain or strong wind).

The micro-locational characteristics of the ARPA-measuring stations and their surrounding urban texture (i.e. distance from major boulevards, height from the ground, prevalence of major boulevards, average width of the streets, presence/absence of canyoning effects due to attached buildings of the same height etc.), instead, do not need to be included among the controls. This is because such characteristics are already inherently perfectly balanced in the estimation procedure, due to the fact that the lockdown L_1 days from any given ARPA station are matched solely with the similar control L_0 days that belong to the same identical ARPA station (i.e. the matching procedure is replicated separately within each of the different ARPA-station multivariate time series, yielding 77 different local ATTs, one for each of the time-series).

The stringency of the lockdown stay-at-home mandate entails that the intensity of fossil-fuel vehicular traffic and other activities was inherently the same between weekends and holidays and the working days during the entire lockdown period L_1. In the baseline control period L_0, before of the Covid-19 lockdown, however, this is not the case, and obvious differences in vehicular traffic intensity were in existence between weekdays and weekends/holidays. In this regard, indeed, a slightly different degree of air-pollution reduction is to be expected based on whether or not the matched L_0 days are working days versus weekends or holidays. Because, in the pre-lockdown period, the working days are more representative of the typical baseline level of fossil-fuel-emitting vehicular traffic and production actives, all the main specifications of the intertemporal MAHD matching, and intertemporal PS and RFR used in the sensitivity analysis, are estimated by limiting the period L_0 to the sole working days of the week.

The specific implementation of the intertemporal MAHD matching is based on a caliper c = 1 which is the value that maximize the statistical efficiency of the analysis under the constrain of satisfying the balancing of the control variables between the intervention days L_1 and the matched controlled days L_0. This latter testing is implemented by means of the Rubin's R and B indices (Rubin 2001, Leuven and Sianesi 2003), with the standard thresholds for acceptance posed in terms of $B < 25$ and $0.5 < R < 2$.

3.3. Heterogeneous-impacts estimation

The estimates from our intertemporal SM model can be conceptualized as being obtained in terms of the difference between a baseline NO_2 pollution recorded under standard pre-lockdown condition and the NO_2 pollution that is recordable in the same identical measuring station, holding everything else constant (including meteorological conditions) except for the abrupt abatement of fossil-fuel traffic brought by the lockdown. In this regard, for each single baseline day, within a same measurement-station time series, it is important to notice that the estimated reduction in NO_2 caused by the fossil fuel traffic abatement has the potential of being different based on the severity of the daily NO_2 pollution. Days with unfavorable meteorological conditions, leading to a buildup of high baseline NO_2 pollution, have a larger potential to greatly benefit from a fossil-fuel traffic abatement than days with favorable meteorological conditions (e.g. windy or rainy conditions).

The Po-river-valley and the central-urban-area location with high traffic density of the measuring stations in our data ensures that the estimated impacts are representative of the average air-quality gain achievable where it matters the most: the places with elevated traffic density and very high average baseline air pollution. In order to further enlarge the external validity of the findings, however, it is also relevant to empirically estimate the NO_2 reduction that may be expected at large in a variety of other urban EU locations exposed to air pollution primarily derived from vehicular traffic. Indeed, outside of the Po-river valley, central urban areas with high traffic-density experience heterogeneous average baseline pollution levels due to different prevailing degrees of favorable meteorological conditions determined by the variation of the orographic locational characteristics which interact with various micro-locational features of the urban texture.

For these reasons it is useful to exploit the whole distribution of the baseline NO_2 pollution recorded in our data (including some low NO_2 levels from the days with heavy precipitations and strong sustained wind, combined with micro locational characteristics of the urban texture less prone to acute NO_2 accumulation), to estimate *heterogeneous impacts* based on categories of the baseline NO_2 pollution. This is achieved by implementing the following intertemporal SM estimation procedure:

I. Holding constant a same measuring station, each lockdown day of L_1 is matched with the baseline (pre-lockdown) day(s) in L_0 with the most similar meteorological characteristics X_t, based on Mahalanobis Distance (MAHD). Likewise for the global ATT estimation, the value of the caliper (c = 1) is determined as the one that maximize the statistical efficiency of the analysis under the constrain of satisfying the balancing of the control variables between intervention days L_1 and matched baseline days L_0.

II. The MAHD matching process (i.e. step I) is repeated for all measurement stations.

III. The paired matched days in L_0 and L_1 are sorted into categories (γ) based on the baseline NO_2 pollution level recorded in L_0. The number and span of these categories are determined with the criteria of covering the entire distribution of the baseline $N0_2$ pollution, ensuring a strong policy relevance of the results, while maintaining also an adequate statistical efficiency of the estimates. This translates into the following eleven categories: 0-10 $\mu g/m^3$; 10-20 $\mu g/m^3$; [.......]; 90-100 $\mu g/m^3$; 100-150 $\mu g/m^3$. For the sensitivity analysis, the estimation is then also repeated with the four categories based on the quartiles of the distribution of the baseline NO_2. This latter solution maximizes the statistical efficiency of the estimates at the expense of reduced policy relevance of the results.

IV. For each day in L_1 on common support, a counterfactual outcome $y_t^{(0)}$ is estimated as the mean of Y of the corresponding matched day(s) from L_0;

V. The categorical intertemporal ATT, for each category γ of baseline pollution, is estimated as the difference of the sample means:

$$\widehat{ATT}_{\gamma} = \frac{1}{n(S_1^{\gamma})} \sum_{t \in S_1^{\gamma}} \left[y_t - \hat{y}_t^{(0)} \right] \tag{9}$$

where S_1^{γ} is the set of the days in L_1 matched with days in L_0 belonging to the category γ of baseline NO_2 pollution;

VI. The estimated categorical $\widehat{ATT_{\gamma}}$ are validated if an adequate balancing is achieved and tested for the covariates X of the days in the intervention period L_1 and those of the matched control days in L_0. Similarly to the estimated average treatment effects, this latter testing is also implemented by means of the Rubin's R and B indices (Rubin 2001, Leuven and Sianesi 2003), with the standard thresholds for acceptance posed in terms of $B < 25$ and $0.5 < R < 2$.

4. Results

This section summarizes the results from our intertemporal SM estimation of the casual effect of Covid-19-lockdown traffic abatement. The reported impact estimates include the average treatment effect on the treated across all the baseline NO_2 pollution levels, a placebo testing involving four different false lockdown periods, heterogeneous impacts based on different categories of baseline NO_2 pollution, and further sensitivity analysis.

4.1. Average treatment effect of lockdown traffic abatement

Tables 3 and 4 illustrates the balancing of the control variables achieved by the intertemporal MAHD SM for the estimation of the average treatment effect on the treated (ATT) across all the daily NO_2 baseline levels. This is in terms of percentage bias and reduction of percentage bias of the pooled distribution (across all the ARPA-stations time series) of the L_1 days and the matched L_0 days (Table 3). For all the control variables, the intertemporal MAHD SM drastically reduces the initial % bias between the intervention period L_1 and the control period L_0. Such reduction in the % bias ranges from 89.6% to 99.2%, with a negligible after-matching remaining % bias which ranges from -0.10% to 2.10%.

Table 3. Balancing of control variables intertemporal MAHD matching (*c* = 1)

Variable	Unmatched/ Matched	Mean Treated	Mean Control	%bias	% reduction |bias|
WIND (m/s)	U	2.13	1.88	19.60	
	M	1.89	1.86	2.00	89.60
RAIN (m/m)	U	1.35	2.43	-17.20	
	M	0.39	0.40	-0.10	99.20
TEMP (c°)	U	13.79	15.05	-20.40	
	M	14.24	14.14	1.60	92.10
WIND-1 (m/s)	U	2.14	1.88	20.30	
	M	1.93	1.90	2.10	89.80
RAIN-1 (m/m)	U	1.34	2.58	-18.90	
	M	0.39	0.41	-0.20	98.70
TEMP-1 (c°)	U	13.71	15.01	-21.10	
	M	13.81	13.70	1.80	91.60

The Rubin's R and B balancing indices are summarized in Table 4. The after-matching values of the B index is 4.1, while that of the R index is 1.01. These values are well within the limits ($B < 25$ and $0.5 < R < 2$) that indicate a fully acceptable overall balancing of the control variables between the intervention days L_1 and the matched controlled days L_0.

Table 4. Rubin's *R* and *B* indices for MAHD matching

Sample	Ps R^2	LR chi^2	$p > chi^2$	Mean Bias	Med Bias	B	R
Unmatched	0.025	659.42	0	19.6	19.9	40.1*	0.77
Matched - MDM	0	3.14	0.792	1.3	1.7	4.1	1.01

Table 5 reports the global ATT impact estimate of the analysis, obtained across all the baseline NO_2 pollution levels. The estimated impact of -13.62 μg/m^3 represents the average reduction in local NO_2 pollution caused by the Covid-19 lockdown. This is in terms of the difference between the baseline NO_2 recorded in the standard working days in the pre-Covid period and the NO_2 recorded in the same exact identical measurement location, holding everything else constant (including all relevant meteorological characteristics), except for the lockdown fossil-fuel traffic abatement. The statistical precision of the ATT point estimate is very high, with a narrow confidence interval (-14.15, -13.09 μg/m^3) and a significance level well within the 5% level.

Table 5. Causal effect of lockdown on NO_2 – global ATT estimates (intertemporal MAHD matching estimates, *c* = 1)

Period	Treated obs. on common support	$\widehat{ATT}$	SE	95% Conf. Interval	
10/03/2020 – 17/05/2020	3,815	-13.62	0.27	-14.15	-13.09

Considering that the average daily baseline NO_2 pollution recorded in 2019 during the same corresponding period of the 2020 Lockdown is about 25.8 μg/m^3 (see Table 1), the estimated ATT impact translate into an average NO_2 reduction of about 53%.

4.2. Placebo test

This section illustrates the results of a placebo test implemented in order to test the robustness of the ATT estimate and to empirically rule out the possibility that same remaining unobservable secular change is responsible for the observed NO_2 reduction, independently from the fossil-fuel traffic abatement of the lockdown. The test is performed by replicating four different times the estimation of our intertemporal MAHD SM estimation, each time assuming as a treatment a different false lockdown periods of the same exact duration but shifted backward from the date of the actual lockdown. This translates into the four different false lockdown periods described in Table 6.

Table 7 summarizes the results of this placebo test. For all of the four false lockdown periods, the estimated average treatment effect (ATT) does not show the presence of a relevant secular trend in the reduction of NO_2. Indeed, for the first false period, which immediately precedes the actual lockdown, the estimated impact is very close to zero (-0.58 μg/m^3) and not statistically significant (at the 5% level). For the remaining three preceding false periods, the ATT point estimates show only a very minimal negative deviation from zero, ranging from -0.70 μg/m^3 for the third period, to -2.71 μg/m^3 for the second period, with statistical significance which barely reaches the 5% level, particularly for the third and, partially, the fourth period.

Table 6. False lockdown periods for the placebo test

Period	Duration (days)	Start date	End Date
Actual lockdown	69	10/03/2020	17/05/2020
False 1	69	01/01/2020	09/03/2020
False 2	69	24/10/2019	31/12/2019
False 3	69	16/08/2019	23/10/2019
False 4	69	08/06/2019	15/08/2019

Table 7: Causal effect of false lockdown on NO_2 level (μg/m³)

False lockdown treatment	Treated obs. on common support	$\widehat{ATT}$	SE	95% Conf. Interval	
False 1 [01/01/2020 – 09/03/2020]	3,232	-0.58	0.36	-1.28	0.12
False 2 [24/10/2019 – 31/12/2019]	2,474	-2.71	0.37	-3.43	-1.98
False 3 [16/08/2019 – 23/10/2019]	3,431	-0.70	0.25	-1.18	-0.22
False 4 [08/06/2019 – 15/08/2019]	3,215	-1.38	0.21	-1.8	-0.97

4.3. Impact heterogeneity based on baseline NO_2

The categorical ATT estimates for the heterogeneous impacts, are reported in both Table 8 and Figure 2. For the days in which the meteorological conditions (combined to favorable micro-locational characteristics of the areas surrounding the measuring station) determine the lowest baseline NO_2 pollution (between 0 and 10 μg/m³), the causal effect of the traffic abatement brought by the lockdown is estimated to be close to zero (-0.18 μg/m³) and not statistically significant (at the 5% confidence).

For the next categories, the magnitude of the reduction of NO_2 pollution caused by the lockdown is estimated to be linearly increasing with the increase of the baseline pollution. These categorical $\widehat{ATT}_{\gamma}$ estimates are always statistical significant and ranges from -4.97 μg/m³, for the 10-20 μg/m³ baseline NO_2 pollution, to a maximum of -62.16 μg/m³ for the highest baseline pollution (100-150 μg/m³).

The linearity of the estimated NO_2 reductions caused by the lockdown translates into quite similar percentages of NO_2 changes for all of the categories above the lowest range of NO_2 baseline pollution (0-10 μg/m³). For the 10-20 μg/m³ category of baseline NO_2, the percentage drop is estimated at around 33%, while for all the remaining categories (from 20-30 μg/m³ to 100-150 μg/m³), the estimated percentage drop is between 43% and 54%.

Figure 2. Lockdown effect by baseline pollution levels (μg/m³)

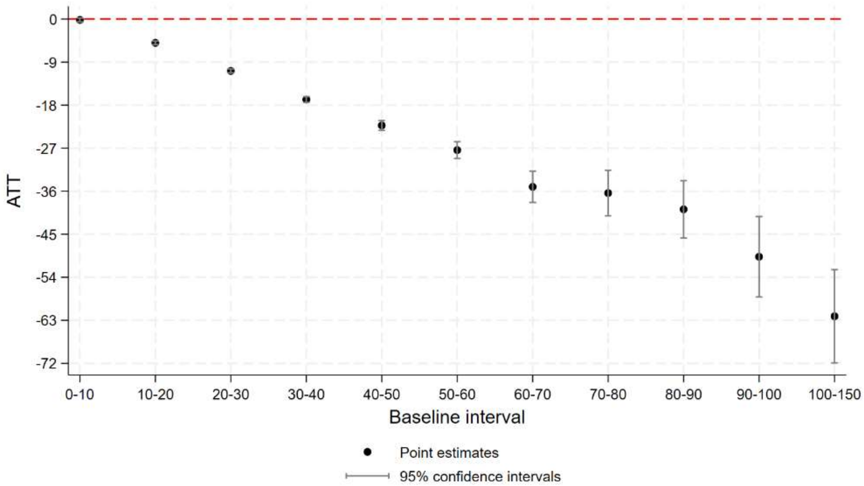

Table 8. Heterogeneous impacts of lockdown based on baseline NO_2

Category γ of baseline NO_2 (μg/m³)	Treated obs. on common support	$\widehat{ATT}_\gamma$	SE	95% Conf. Interval	
0 - 10	369	-0.18	0.21	-0.59	0.23
10 - 20	948	-4.97	0.19	-5.34	-4.59
20 - 30	837	-10.83	0.22	-11.26	-10.40
30 - 40	794	-16.83	0.32	-17.45	-16.21
40 - 50	406	-22.24	0.53	-23.28	-21.19
50 - 60	233	-27.40	0.89	-29.15	-25.65
60 - 70	91	-35.08	1.67	-38.35	-31.80
70 - 80	62	-36.38	2.42	-41.13	-31.63
80 - 90	34	-39.79	3.06	-45.79	-33.80
90 - 100	18	-49.71	4.29	-58.12	-41.30
100 - 150	22	-62.16	4.97	-71.91	-52.41

4.4. Sensitivity analysis

In addition to the placebo testing, the robustness of our average treatment effect results is further assessed by replicating the analysis with different specifications of Mahalanobis Distance (MAHD), a number of intertemporal Propensity Score (PS) matching models, and a Random Forest Regression (RFR) approach. Although our main estimation model, in terms of intertemporal MAHD matching with caliper c = 1, is a preferable option because it maximizes statistical efficiency under the constrain of a stringent balancing of the control variables, other intertemporal MAHD and PS matching specifications are also applicable, as they still ensure a sufficient balancing of the controls. The alternative intertemporal matching specifications, used in our sensitivity analysis, are: MAHD matching with caliper c = 1.5; MAHD matching with no caliper (i.e. nearest neighbour MAHD matching); nearest neighbour PS matching with caliper 0.1; and radius PS matching with calipers 0.02, 0.05 and 0.1.

The RFR estimation, finally, is also included in the sensitivity analysis for assessing how the results from our intertemporal SM compare with respect to another emerging causal-inference strategy that has been adopted in the literature on Covid-19 lockdowns and air-pollution time-series data (e.g. Grange et al. 2018, Lovrić et al. 2021). Similar to the intertemporal SM approach, our RFR estimation is applied separately to each measuring-station multivariate time series data, yielding a different local impact (ATT) estimate for each measuring-station time series. The local ATTs are then averaged-out into a global ATT estimate.[19] The training period of our RFR model is the same control period L_0 (training set) used for the intertemporal PS and MAHD matching, while the predicted NO_2 values for the days in the period L_1 (intervention) represent the counterfactual estimates for each of the lockdown days. The local ATTs for each of the ARPA station time-series are then estimated as the average difference between the observed and predicted NO_2 values for the L_1 days.

[19] RFR (Breiman 2001) is performed using the module *rforest* of Stata (Schonlau and Zou 2020).

Table 9. ATT estimates under different MAHD and PS matching specifications and Random Forest Regression

Method	$\widehat{ATT}$	SE	95% Conf. Interval	
MAHD intertemporal matching (caliper = 1.5)	-13.33	0.24	-13.81	-12.86
MAHD intertemporal matching (no caliper)	-13.77	0.22	-14.21	-13.33
PS intertemp. *nearest neighbour* matching (caliper = 0.1)	-14.90	0.30	-15.49	-14.32
PS intertemp. *radius* matching (caliper = 0.02)	-13.11	0.19	-13.47	-12.74
PS intertemp. *radius* matching (caliper = 0.05)	-13.32	0.17	-13.66	-12.98
PS intertemp. *radius* matching (caliper = 0.1)	-13.79	0.16	-14.11	-13.47
Random Forest Regression	-13.45	0.12	-13.67	-13.22

The results from this wide range of sensitivity analyses (Table 9), comfortingly, confirm the robustness of our main findings.

For the heterogeneous-impact analysis, the number and the span of the discrete-interval categories adopted in the main intertemporal MAHD matching estimation have been optimized to cover in detail the entire distribution, and to ensure strong policy relevance of the results. In terms of sensitivity analysis, however, it is useful to test other alternative heterogeneity specifications, such as an operationalization of the categories of baseline NO_2 based on the quartile of the distribution. This latter specification has the advantage of maximizing the statistical efficiency of the estimates, albeit at the expense of policy-relevance, and it is added to the sensitivity analysis, in order to test the robustness of the main-specification results.

Table 10. Heterogeneous impacts based on quartiles of baseline NO_2

Quartiles Q of baseline NO_2	$\widehat{ATT}_Q$	SE	95% Conf. Interval	
$Q1$ = [$\leq$ 16.85] µg/m3	-2.69	0.17	-3.02	-2.37
$Q2$ = [16.85, 27.07] µg/m3	-8.70	0.17	-9.03	-8.37
$Q3$ = [27.07, 38.56] µg/m3	-15.56	0.25	-16.05	-15.07
$Q4$ = [> 38.56] µg/m3	-27.43	0.45	-28.31	-26.56

The results from this sensitivity analysis (Table 10 and Figure 3) fully confirm the findings from the main MAHD specification. There is a monotonic increase in the magnitude of the point estimates, from the first to the fourth quartile of the baseline NO_2, which ranges from -2.69 µg/m^3 (first quartile), to -27.43 µg/m^3 (fourth quartile). Similar to the discrete-interval categorical impacts from the main specification, such increasing magnitude of the estimated NO_2 reduction highlight a linear trend, when moving from the lowest to highest NO_2 baseline pollution.

Figure 3. Lockdown effect by baseline quartile pollution levels (μg/m³)

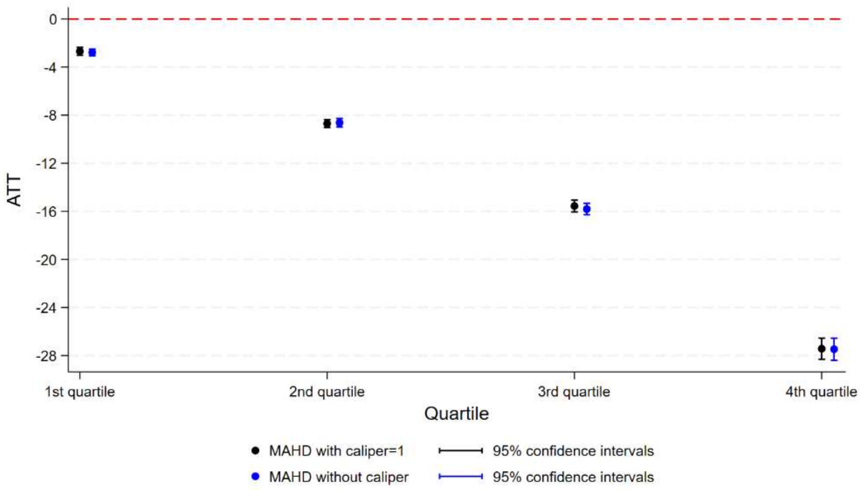

5. Translation of NO_2 reduction into health outcomes

Translating the estimated NO_2 reductions potentially produced by future regulations, such as the EU Zero-Emission-Vehicles Resolution, into health benefits is important for several reasons. First, it serves as a powerful tool for informing and engaging various stakeholders in efforts to improve air quality and public health and for providing policymakers with evidence to support the implementation of stricter regulations and targeted interventions. Second, it enables the implementation of cost-benefit analyses, allowing decision-makers to prioritize actions that offer the greatest return on investment in terms of public health, facilitating the setting of specific targets for NO_2 reduction and guiding regulatory agencies and industries in their efforts to mitigate pollution and track progresses over time. Third, it can help mobilize public support for environmental policies and regulations, because individuals become more aware of the direct impact of cleaner air on their health and well-being. Forth, it underscores the need for equity considerations in policymaking, drawing attention to the disproportionate burden of air pollution on vulnerable populations and advocating for interventions that prioritize the health and well-being of all communities.

Due to the strong consensus in the medical literature about the long-term effects on mortality associated with exposure to NO_2 pollution, our computation of the health benefits of NO_2 reduction is focused on mortality gains. Indeed, among others, Faustini et al. (2014) have analyzed 23 studies published between 2004 and 2013, performing a random-effects meta-analysis in order to evaluate the link between NO_2 and mortality. The evidence from this meta-analysis suggests that, for Europe, the pooled estimates of NO_2 effects, per 10 μg/m³, on total mortality are a Relative Risk (RR) of 1.066 (95% CI: 1.029–1.104), while those for cardiovascular and respiratory mortality are RR 1.059 (95% CI: 1.032–1.086) and RR 1.029 (95% CI: 1.013–1.045), respectively.

These parameters can be usefully applied to our estimated NO_2 reduction caused by Covid-19 lockdown fossil-fuel-traffic abatement, which mimics the future scenario of 2035 EU Zero-Emission-Vehicles Resolution. In particular, by assuming a linear relationship between NO_2 exposure and total and cause-specific RR of mortality, based on Faustini et al. (2014), our estimated average reduction of -13.6 μg/m³ in the daily NO_2 pollution caused by the lockdown translates into a decrease of the relative risk of total mortality of about 9%, while the estimated benefit for the cardiovascular and respiratory mortality is about 8% and 4%, respectively.

Table 11. Reductions of mortality RR associated with estimated NO_2 impacts (ATT)

Category γ of baseline NO_2 ($\mu g/m^3$)	$\widehat{ATT}_\gamma$	RR total mortality (%)	RR cardiovascular mortality (%)	RR respiratory mortality (%)
0 - 10	-0.18	-0.12	-0.11	-0.05
10 - 20	-4.97	-3.28	-2.93	-1.44
20 - 30	-10.83	-7.15	-6.39	-3.14
30 - 40	-16.83	-11.11	-9.93	-4.88
40 - 50	-22.24	-14.68	-13.12	-6.45
50 - 60	-27.40	-18.08	-16.17	-7.95
60 - 70	-35.08	-23.15	-20.70	-10.17
70 - 80	-36.38	-24.01	-21.46	-10.55
80 - 90	-39.79	-26.26	-23.48	-11.54
90 - 100	-49.71	-32.81	-29.33	-14.42
100 - 150	-62.16	-41.03	-36.67	-18.03

Notes: Authors' computations based on parameters from Faustini et al. (2014).

Given the heterogeneity of our estimated impacts of the Covid-19 lockdown based on the different levels of baseline NO_2 pollution, it is important to consider that these health benefits are likely to have an uneven spatial distribution across EU urban areas. This is due to different prevailing meteorological daily characteristics, combined with different local urban texture features, which determine different average baseline NO_2 pollution levels in the European central urban areas exposed to elevated fossil-fuel vehicular traffic. Indeed, our empirical evidence shows that when the baseline NO_2 pollution is extremely low (i.e. from 0 to 10 $\mu g/m^3$), the estimated impact of the fossil-fuel-traffic abatement is negligible, with ensuing insignificant air-improvement health benefits (Table 11). When instead the baseline NO_2 pollution is higher and fall in the second category (10-20 $\mu g/m^3$), the estimated NO_2 reduction translates into health benefits in the order of -3.3% for the RR of total mortality and of -2.9% and -1.4% for the RR of cardiovascular mortality and respiratory mortality, respectively. Likewise, for each subsequent interval of higher baseline NO_2 pollution considered in our analysis, the linearly-increasing estimated NO_2 reductions translate into progressively higher health benefits. These reaches a maximum RR reduction of about 41%, 37% and 18%, for total, cardiovascular and respiratory mortality, respectively, when the baseline $N0_2$ pollution is within the highest interval of 100-150 $\mu g/m^3$. All of these dose-specific estimated RR gains are computed on the assumption of a strict linear relationship between nitrogen dioxide exposure and health outcomes. This is because, although the evidence in the medical literature is more indicative of a concave positively-sloped dose response function linking NO_2 exposure to health outcomes (e.g., Künzli 2002), no robustly-tested parameters (outside of those from Faustini et al. 2014) can be readably used for the RR computations to account for concavities and/or thresholds or nonlinear jumps where negative health impacts accelerate at higher NO_2 concentrations.

Assuming a linearity link between dioxide exposure and health outcomes, when instead the true relationship may be indeed concave and/or with non-linear accelerations, however, can be usefully regarded as a robust lower-bound estimate of the health impacts associated with reductions in NO_2 exposure. As a consequence, our dose-specific estimations of Table 11 represent a safe conservative approach to inform public health officials and policy makers about the minimum certain health benefits that are locally achievable from air quality improvements, stimulated in central urban areas by a sharp abatement of fossil-fuel vehicular traffic at different levels of baseline NO_2.

6. Concluding remarks

Covid-19 pandemic and related lockdowns have greatly improved outdoor air quality in regions across the world (e.g. Dang and Trinh 2021, Huang et al. 2021, Blackman et al. 2023). Also driving restrictions are proven by the literature to be correlated with remarkable air quality improvements in urban areas (Gibson and Carnovale 2015, Luechinger and Roth 2016, Han et al. 2020, Green et al. 2020, Domon et al. 2022). Moreover, the harmful effects of the exposure to air pollutants is a well debated topic in the literature, given the adverse impact not only on hospital admissions (Lagravinese et al. 2014) and health status (Faustini et al. 2014), but also on other important socio-economic outcomes including school performances (Currie et al. 2009b), human capital (Graff Zivin and Neidell 2013), labour supply (Hanna and Oliva 2015), and social welfare (Proost and Van Dender 2001). Therefore, long-lasting air quality improvements may have long-term benefits and make citizens more sensitive to the presence of chronic air pollution, especially in highly congested urban areas, thus increasing political pressure for effective environmental reforms. For this reason, empirical evaluations of policies aimed at-improving urban air-quality will increasingly gain importance. In this regard, the first contribution offered by this study is the development (building on Bondonio and Chirico 2024) of a novel counterfactual impact evaluation tool, in terms of an intertemporal statistical matching (SM) approach which is specifically suited for the unique identification conditions posed by these policies.

By applying our novel intertemporal SM approach and leveraging the unique conditions of the Italian Covid-19 lockdown as a natural-experiment for an exogenous fossil-fuel traffic abatement in urban areas with elevated traffic density, the second contribution of this study is to offer evidence on the reduction in urban NO_2 pollution (and related health outcomes gains) that might be expected from the implementation of the EU 2035 zero-emission-mobility resolution. In this regard, our results show that the fossil-fuel traffic abatement brought by the Italian lockdown caused an average NO_2 reduction of 13.62 $\mu g/m^3$, representing about a 53% decrease from baseline values.

Exploiting data from a large sample of air-pollution measuring stations (which provides a wide-spread distribution of the baseline NO_2 pollution determined by varying daily meteorological conditions and local urban texture features), our analysis also estimates heterogeneous NO_2 impacts based on different baseline pollution levels. This is a critical aspect often overlooked in other studies, as the magnitude of the NO_2 reduction may crucially differ based on different degrees of baseline NO_2 concentrations. In this regard, our results indicate that, indeed, the NO_2 reductions caused by fossil-fuel traffic abatement increase (almost linearly) along with increments of the baseline NO_2 concentration, with estimates ranging from -0.18 $\mu g/m^3$ for the least polluted conditions to -62.16 $\mu g/m^3$ for the most polluted ones.

These local air-quality gains translate into significant health benefits which can be estimated in terms of a 9% average decrease in the relative risk of mortality for all causes, with even more pronounced health benefits when considering the NO_2 reduction for the highest baseline pollution conditions. These latter results indicate that the regions with meteorological conditions and typical urban texture features that exacerbate NO_2 accumulation stand to benefit disproportionately from stringent vehicular emission controls, suggesting the need for tailored policy approaches that account for local environmental conditions. Indeed, our heterogeneous NO_2 impact estimates support a nuanced application of these policies, with high-pollution areas that could be prioritized for intervention, potentially through more aggressive timelines or additional support measures to accelerate the transition. Less polluted areas could be instead considered for more generous fossil-fuel traffic phasing-out periods and allowances.

Taken together, our methodological contribution and findings provide an important piece of empirical evidence in the debate surrounding the EU zero-emission mobility resolution. This is by highlighting the estimated health benefit from local pollution gains in urban areas, a significant element which is often neglected and it's suggestive of potentially relevant policy implications. This contribution importantly complements the other factors that are usually discussed and weighted in the literature (e.g. Peszko et al. 2023; Holm Møller et al. 2019; Zipper 2023; Krishnan 2022) when assessing zero-emission mobility proposals. Noticeably: the need to examine the entire lifecycle emissions of zero-emission vehicles, including electricity generation; the welfare loss due to drastic changes in the European automotive industry and its supply chain; the opportunity cost of taxpayers' money needed to implement the infrastructures for the zero-emission mobility transition; the risk of displacing resources available to public transit system improvements for the promotion of private electric vehicles usage; and the loss of welfare, particularly for the groups of less affluent citizens, related to the higher purchasing cost of electric vehicles.

References

Abrate, G., Piacenza, M., Vannoni, D. (2009). The impact of Integrated Tariff Systems on public transport demand: Evidence from Italy. *Regional Science and Urban Economics*, 39(2), 120-127.

Agarwal, N., Banternghansa, C., Bui, L. T. (2010). Toxic exposure in America: Estimating fetal and infant health outcomes from 14 years of TRI reporting. *Journal of health economics*, *29*(4), 557-574.

Agresti, V., Balzarini, A., Bonanno, R., Collino, E., Colzi, F., Lacavalla, P. M., Piccoli, A. (2020). Gli effetti del lockdown sulla qualitá dell'aria a Milano e in Lombardia. *Report*. (https://dossierse.it/05-2020-gli-effetti-del-lockdown-sulla-qualita-dellaria-a-milano-e-in-lombardia).

Ahlfeldt, G.M., Pietrostefani, E. (2019). The economic effects of density: A synthesis. *Journal of Urban Economics*, *111*, 93-107.

Almond, D., Du, X., Karplus, V. J., Zhang, S. (2021, May). Ambiguous air pollution effects of China's COVID-19 lock-down. In *AEA Papers and Proceedings* (Vol. 111, pp. 376-380).

Anil, I., Alagha, O. (2020). The impact of COVID-19 lockdown on the air quality of Eastern Province, Saudi Arabia. *Air Quality, Atmosphere and Health*, 14: 117–128.

Arneodo, F., Castelli R., Cerboni, G, (2021) Analisi impatti della Pandemia sulla mobilità. *Politiche Piemonte. L'impatto Covid in Piemonte*, n. 68, pp. 27-35, IRES Piemonte (https://www.ires.piemonte.it/index.php/news/231-2021/1121-politiche-piemonte-n-68-l-impatto-covid-in-piemonte).

Anttila, P., Tuovinen, J.P., Niemi, J.V., (2011). Primary NO2 emissions and their role in the development of NO2 concentrations in a traffic environment. *Atmospheric Environment* 45, 986–992.

Arregocés, H.A., Rojano, R., Restrepo, G. (2021). Impact of lockdown on particulate matter concentra_ tions in Colombia during the COVID-19 pandemic. *Science of The Total Environment*, 764, 142874.

Auffhammer, M., Kellogg, R. (2011). Clearing the air? The effects of gasoline content regulation on air quality. *Am. Econ. Rev.* 101 (6), 2687–2722.

Bachtiar, V.S., Purnawan, P., Afrianita, R., Ritonga, S.H. (2017). Modelling of NO2 dispersion based on receptor position due to transport sector in Padang city, Indonesia. *Journal of Environmental Science and Technology 10 (5): 258-267.*

Barreca, A.I., Matthew N., Sanders N.J. (2021). Long-run pollution exposure and mortality: Evidence from the Acid Rain Program. *Journal of Public Economics*, 200, 104440.

Barron, M, Torero, M. (2017). Household electrification and indoor air pollution. *Journal of Environmental Economics and Management*, 86: 81-92.

Bell, M.L., Dominici, F., Samet. J.M. (2005). A meta-analysis of time-series studies of ozone and mortality with comparison to the national morbidity, mortality, and air pollution study. *Epidemiology*, 16.4: 436.

Bento, A., Kaffine, D., Roth, K., Zaragoza-Watkins, M. (2014). The effects of regulation in the presence of multiple unpriced externalities: Evidence from the transportation sector. *American Economic Journal: Economic Policy*, 6(3), 1-29.

Blackman, A., Bonilla, J.A., Villalobos, L. (2023). Quantifying COVID-19's silver lining: Avoided deaths from air quality improvements in Bogotá. Journal of environmental economics and management, 117, 102749.

Bondonio D. (2022). Does the Running Variable Matter? A Second Look at Discontinuity Designs for Evaluating Regional Economic Development and Business Incentive Policies, *Evaluation Review*, 46 (5): 598-625.

Bondonio D., Chirico P. (2024). Intertemporal propensity score matching for casual inference: an application to covid-19 lockdowns and air pollution in Northern Italy, in *Advanced Methods in*

Statistics, Data Science and Related Applications, (eds: Bini M., Balzanella L., Masserini L., Verde R.), Springer ISBN: 978-3-031-65698-9

Borck, R., Schrauth, P. (2021). Population density and urban air quality. *Regional Science and Urban Economics*, 86: 103596.

Borck, R. (2019). Public transport and urban pollution". *Regional Science and Urban Economics*, 77 (2019): 356-366.

Breiman, L. (2001). Random forests. *Machine learning*, 45(1), 5-32

Brodeur, A., Cook, N., Wright, T. (2021). On the effects of COVID-19 safer-at-home policies on social distancing, car crashes and pollution. *Journal of environmental economics and management*, *106*, 102427.

Carozzi, F., Roth, S. (2023). Dirty density: air quality and the density of American cities. *Journal of Environmental Economics and Management* 118: 102767.

Carslaw, D.C., Farren, N.J., Vaughan, A.R., Drysdale, W., Young, S., Lee, J.D. (2019). The diminishing importance of nitrogen dioxide emissions from road vehicle exhaust. *Atmospheric Environment: X*, *1*, 100002.

Chaney A.M., Cryer D.J., Nicholl E.J., Seakins P.W. (2011). NO and NO2 interconversion downwind of two different line sources in suburban environments". *Atmospheric Environment* 45: 5863-5871

Chen, S., Jiang, L., Liu, W., Song, H. (2022). Fireworks regulation, air pollution, and public health: Evidence from China. *Regional Science and Urban Economics*, *92*, 103722.

Chen, Y., Whalley, A. (2012). Green infrastructure: The effects of urban rail transit on air quality. *American Economic Journal: Economic Policy*, *4*(1), 58-97.

Chen, Z., Hao, X., Zhang, X., Chen, F. (2021). Have traffic restrictions improved air quality? A shock from COVID-19. *Journal of cleaner production*, *279*, 123622.

Coker E.S, Cavalli L., Fabrizi E., Guastella G., Lippo E., Parisi M.L., Pontarollo N., Rizzati M., Varacca A., Vergalli S. (2020). The Effects of Air Pollution on COVID-19 Related Mortality in Northern Italy. *Environmental and Resource Economics* 76:611–634.

Collivignarelli, M. C., Abba, A., Bertanza, G., Pedrazzani, R., Ricciardi, P., Miino, M. C. (2020) Lockdown for CoViD-2019 in Milan: What are the effects on air quality? *Science of the total environment*, 732, 139280.

Currie, J., Neidell, M. (2005). Air pollution and infant health: what can we learn from California's recent experience?. *The quarterly journal of economics*, *120*(3), 1003-1030.

Currie, J., Neidell, M., Schmieder, J.F., (2009). Air pollution and infant health: lessons from New Jersey. *Journal of Health Economics.* 28, 688–703.

Currie, J., Hanushek, E.A., Kahn, E.M., Neidell, M., Rivkin, S.G. (2009). Does pollution increase school absences?. *The Review of Economics and Statistics*, *91*(4), 682-694.

Dang, H.A.H., Trinh, T.A. (2021). Does the COVID-19 lockdown improve global air quality? New cross-national evidence on its unintended consequences. *Journal of Environmental Economics and Management*, *105*, 102401.

Davis, L.W. (2008). The effect of driving restrictions on air quality in Mexico City. *Journal of Political Economy*, *116*(1), 38-81..

Dehejia, R.H., Wahba, S. (2002) Propensity score-matching methods for non experimental causal studies. *Review of Economics and statistics*, 84(1), 151-161.

Deschenes, O., Greenstone, M., Shapiro, J.S. (2017). Defensive investments and the demand for air quality: Evidence from the NOx budget program. *American Economic Review*, *107*(10), 2958-2989..

Dominici, F., Peng, R.D., Bell, M.L., Pham, L., McDermott, A., Zeger, S.L., Samet, J.M. (2006). Fine particulate air pollution and hospital admission for cardiovascular and respiratory diseases. *Jama*, *295*(10), 1127-1134.

Domon, S., Hirota, M., Kono, T., Managi, S., Matsuki, Y. (2022). The long-run effects of congestion tolls, carbon tax, and land use regulations on urban CO2 emissions. *Regional Science and Urban Economics*, *92*, 103750..

EEA (2022): *Air quality in Europe* 2022. Report no. 05/2022

Faustini, A., Rapp, R., Forastiere, F. (2014). Nitrogen dioxide and mortality: review and meta-analysis of long-term studies. *European Respiratory Journal*, *44*(3), 744-753.

Meredith L., 2009. Incomplete environmental regulation, imperfect competition, and emissions leakage. *Am. Econ. J. Econ. Pol.* 1 (2), 72–112.

Fu, S., and Yizhen G. (2017). Highway toll and air pollution: Evidence from Chinese cities. *Journal of environmental Economics and Management* 83: 32-49.

Gallego, F., Montero, J.P., Salas, C. (2013). The effect of transport policies on car use: Evidence from Latin American cities. *Journal of Public Economics*, *107*, 47-62.

Gehrsitz, M. (2017). The effect of low emission zones on air pollution and infant health. *Journal of Environmental Economics and Management*, *83*, 121-144.

Gendron-Carrier, N., Gonzalez-Navarro, M., Polloni, S., Turner, M.A. (2022). Subways and urban air pollution. *American economic journal: Applied economics*, *14*(1), 164-196.

Ghasempour, F., Sekertekin, A., Kutoglu, S.H. (2021). Google Earth Engine based spatio-temporal analysis of air pollutants before and during the first wave COVID-19 outbreak over Turkey via remote sensing. *Journal of Cleaner Production*, *319*, 128599..

Gibson, M., Carnovale, M. (2015). The effects of road pricing on driver behavior and air pollution." *Journal of Urban Economics* 89: 62-73.

Graff Zivin, J., Neidell, M. (2013). Environment, health, and human capital. *Journal of economic literature*, *51*(3), 689-730.

Graff Zivin, J., Neidell, M. (2009). Days of haze: Environmental information disclosure and intertemporal avoidance behavior. *Journal of Environmental Economics and Management*, *58*(2), 119-128.

Grange, S.K., Carslaw, D.C., Lewis, A.C., Boleti, E., Hueglin, C. (2018). Random forest meteorological normalisation models for Swiss PM10 trend analysis. *Atmospheric Chemistry and Physics*, 18(9), 6223-6239

Green, C.P., Heywood, J.S., Navarro Paniagua, M. (2020). Did the London congestion charge reduce pollution? *Regional Science and Urban Economics, 84*, 103573.

Greenstone, M., Hanna, R. (2014). Environmental regulations, air and water pollution, and infant mortality in India. *American Economic Review, 104*(10), 3038-3072.

Gu, Y., Deakin, E., Long, Y. (2017). The effects of driving restrictions on travel behavior: Evidence from Beijing. *Journal of Urban Economics, 102*, 106-122.

Gualtieri, G., Brilli, L., Carotenuto, F., Vagnoli, C., Zaldei, A., Gioli, B. (2020). Quantifying road traffic impact on air quality in urban areas: A Covid-19-induced lockdown analysis in Italy. *Environmental Pollution, 267*, 115682.

Han, Q., Liu, Y., Lu, Z. (2020). Temporary driving restrictions, air pollution, and contemporaneous health: Evidence from China. *Regional Science and Urban Economics, 84*, 103572.

Hanna, R., Oliva, P. (2015). The effect of pollution on labor supply: Evidence from a natural experiment in Mexico City. *Journal of Public Economics, 122*, 68-79.

He, G., Pan, Y., Tanaka, T. (2020). The short-term impacts of Covid-19 lockdown on urban air pollution in China. *Nature Sustainability, 3*(12), 1005-1011.
Hilber, C. A. L., Palmer, C. (2014). Urban development and air pollution: Evidence from a global panel of cities. *Grantham Research Institute on Climate Change and the Environment Working Paper series*.
Holland, S.P., Mansur, E.T., Muller, N.Z., Yates, A.J. (2016). Are there environmental benefits from driving electric vehicles? The importance of local factors. *American Economic Review, 106*(12), 3700-3729.
Holm Møller, T., Simlett, J., Mugnier, E. (2019). Micromobility: Moving cities into a sustainable future. *Ernst & Young Report*.
Huang, X., Ding, A., Gao, J., Zheng, B., Zhou, D., Qi, X., He, K. (2021). Enhanced secondary pollution offset reduction of primary emissions during COVID-19 lockdown in China. *National Science Review*, *8*(2), nwaa137.
Iacus, S.M., King, G., Porro, G. (2011). Multivariate matching methods that are monotonic imbalance bounding. *Journal of the American Statistical Association, 106*(493), 345-361.
Isaksen, E.T. (2020). Have international pollution protocols made a difference? *Journal of Environmental Economics and Management, 103*, 102358.
ISPRA. (2021). Italian Emission Inventory 1990-2019. Informative Inventory Report 2021. Roma, IT: Istituto Superiore per la Sicurezza e la Ricerca Ambientale.
Isprambiente. (2022). Il parco autovetture nazionale: rinnovo e sostenibilità in La mobilità sostenibile nelle aree urbane: la situazione attuale e le prospettive future. ACI, Roma.
Jayaraman, G. (2008). Air pollution and associated respiratory morbidity in Delhi. *Health Care Management Science, 11*, 132-138.
Jerrett, M., Buzzelli, M., Burnett, R. T., De Luca, P. F. (2005). Particulate air pollution, social confounders, and mortality in small areas of an industrial city. *Social science & medicine*, *60*(12), 2845-2863.
Knittel, C. R., Miller, D. L., Sanders, N. J. (2016). Caution, drivers! Children present: Traffic, pollution, and infant health. *Review of Economics and Statistics, 98*(2), 350-366.
Krishnan, M. (2022). The anatomy of net-zero transition. *Project Syndicate*.
Künzli, N. (2002). The public health relevance of air pollution abatement. *European Respiratory Journal, 20*(1), 198-209.
Lagravinese, R., Moscone, F., Tosetti, E., Lee, H. (2014). The impact of air pollution on hospital admissions: evidence from Italy. *Regional Science and Urban Economics*, *49*, 278-285.
Lalive, R., Luechinger, S., Schmutzler, A. (2018). Does expanding regional train service reduce air pollution? *Journal of Environmental Economics and Management, 92*, 744-764.
Leuven, E., Sianesi, B. (2003). PSMATCH2: Stata module to perform full Mahalanobis and propensity score matching, common support graphing, and covariate imbalance testing.
Li, P., Lu, Y., Wang, J. (2020). The effects of fuel standards on air pollution: Evidence from China. *Journal of Development Economics, 146*, 102488.
Lleras-Muney, A. (2010). The needs of the army: Using compulsory relocation in the military to estimate the effect of air pollutants on children's health. *Journal of Human Resources, 45*(3), 549-590
Lovrić, M., Pavlović, K., Vuković, M., Grange, S. K., Haberl, M., Kern, R. (2021). Understanding the true effects of the COVID-19 lockdown on air pollution by means of machine learning. *Environmental Pollution, 274*, 115900.
Luechinger, S., Roth, F. (2016). Effects of a mileage tax for trucks. *Journal of Urban Economics, 92*, 1-15.
Mayeres, I., Proost, S. (2001). Should diesel cars in Europe be discouraged? *Regional Science and Urban Economics, 31*(4), 453-470.

Moretti, E., Neidell, M. (2011). Pollution, health, and avoidance behavior: evidence from the ports of Los Angeles. *Journal of Human Resources, 46*, 154–175.

Nafstad, P., Håheim, L. L., Wisløff, T., Gram, F., Oftedal, B., Holme, I., Leren, P. (2004). Urban air pollution and mortality in a cohort of Norwegian men. *Environmental health perspectives*, *112*(5), 610-615.

Namdeo, A., Tiwary, A., Farrow, E. (2011). Estimation of age-related vulnerability to air pollution: assessment of respiratory health at local scale. *Environment International, 37*(5), 829-837.

Neidell, M. J. (2004). Air pollution, health, and socio-economic status: the effect of outdoor air quality on childhood asthma. *Journal of Health Economics, 23*(6), 1209-1236.

Palmgren, F., Berkowitz, R., Hertel, O., Vignati, E. (1996). Effects of reduction of NOx on the NO2 levels in urban streets. *Science of the Total Environment, 189*, 409-415.

Parry, I. W. H., Timilsina, G. R. (2010). How should passenger travel in Mexico City be priced? *Journal of Urban Economics, 68*(2), 167-182.

Parry, I. W. H. (2007). Are the costs of reducing greenhouse gases from passenger vehicles negative? *Journal of Urban Economics, 62*(2), 273-293.

Pestel, N., Wozny, F. (2021). Health effects of low emission zones: evidence from German hospitals. *Journal of Environmental Economics and Management, 109*, 102512.

Peszko, G., Amann, M., Awe, Y., Kleiman, G., Rabie, T. S. (2023). *Air Pollution and Climate Change: From Co-Benefits to Coherent Policies*. World Bank Group.

Portney, P. R., Mullahy, J. (1986). Urban air quality and acute respiratory illness. *Journal of Urban Economics, 20*(1), 21-38.

Portney, P. R., Mullahy, J. (1990). Urban air quality and chronic respiratory disease. *Regional Science and Urban Economics, 20*(3), 407-418.

Proost, S., Van Dender, K. 82001), The welfare impacts of alternative policies to address atmospheric pollution in urban road transport. *Regional Science and Urban Economics, 31*(4), 383-411.

Rangel, M. A., Vogl, T. S. (2019). Agricultural fires and health at birth. *Review of Economics and Statistics, 101*(4), 616-630.

Rava, M., Marcon, A., Girardi, P., Pironi, V., Silocchi, C., Ricci, P., De Marco, R. (2011). Proximity to wood factories and hospitalizations for respiratory diseases in children. *Science of the total environment*, *410*, 80-86.

Restrepo, C. E. (2021). Nitrogen dioxide, greenhouse gas emissions and transportation in urban areas: lessons from the Covid-19 pandemic. *Frontiers in Environmental Science, 9*, 689985.

Rivera, N. M. (2021). Air quality warnings and temporary driving bans: Evidence from air pollution, car trips, and mass-transit ridership in Santiago. *Journal of Environmental Economics and Management, 108*, 102454.

Rosenbaum, P. R., Rubin, D. B. (1983). The central role of the propensity score in observational studies for causal effects. *Biometrika, 70*(1), 41–55.

Rubin, D. B. (2001). Using propensity scores to help design observational studies: application to the tobacco litigation. *Health Services and Outcomes Research Methodology, 2*(3), 169–188.

Samakovlis, E., Huhtala, A., Bellander, T., Svartengren, M. (2005). Valuing health effects of air pollution - focus on concentration-response functions. *Journal of Urban Economics*, *58*(2), 230-249.

Seo, J. H., Jeon, H. W., Sung, U. J., Sohn, J. R. (2020). Impact of the COVID-19 outbreak on air quality in Korea. *Atmosphere, 11*(10), 1137.

Song, Y., Li, Z., Liu, J., Yang, T., Zhang, M., Pang, J. (2021). The effect of environmental regulation on air quality in China: A natural experiment during the Covid-19 pandemic. *Atmospheric Pollution Research, 12*(4), 21–30.

Stuart, E. A. (2010). Matching methods for causal inference: A review and a look forward. *Statistical Science: A Review Journal of the Institute of Mathematical Statistics, 25*(1).

Sun, C., Xu, S., Yang, M., Gong, X. (2022). Urban traffic regulation and air pollution: A case study of urban motor vehicle restriction policy. *Energy Policy, 163*, 112819.

Veza I., Zacky Asy'ari, M., Idris M., Epin V., Fattah, I.M.R., Spraggon, M. (2023). Electric vehicle (EV) and driving towards sustainability: Comparison between EV, HEV, PHEV, and ICE vehicles to achieve net zero emissions by 2050 from EV". *Alexandria Engineering Journal* 82: 459–467.

Viard, V. Brian, and Shihe Fu. (2018). The effect of Beijing's driving restrictions on pollution and economic activity." *Journal of Public Economics* 125: 98-115.

Wang, J., Xu, X., Wang, S., He, S., He, P. (2021). Heterogeneous effects of Covid-19 lockdown measures on air quality in northern china. *Applied Energy* 282:116–179.

Wang, Kunlun, Hongchun Yin, and Yiwen Chen. (2019). The effect of environmental regulation on air quality: A study of new ambient air quality standards in China." *Journal of Cleaner Production* 215: 268-279.

WHO Europe (2006). *Air quality guidelines for particulate matter, ozone, nitrogen dioxide and sulfur dioxide. Global update 2005*. Geneva, World Health Organization.

Wolff, H. (2014). Keep your clunker in the suburb: low-emission zones and adoption of green vehicles. *Economic Journal.* 124 (578), F481–F512.

Zhang, R., Li, H., Khanna, N. (2021). Environmental justice and the COVID-19 pandemic: Evidence from New York State. *Journal of environmental economics and management*, *110*, 102554.

Zipper, D. (2023) *Why Norway – the poster child for electric cars – is having second thoughts*. Vox